AIP | Journal of Applied Physics

# Cathodoluminescence microscopy and spectroscopy of GaN epilayers microstructured using surface charge lithography

C. Díaz-Guerra, J. Piqueras, O. Volciuc, V. Popa, and I. M. Tiginyanu

Citation: J. Appl. Phys. **100**, 023509 (2006); doi: 10.1063/1.2214210
View online: http://dx.doi.org/10.1063/1.2214210
View Table of Contents: http://jap.aip.org/resource/1/JAPIAU/v100/i2
Published by the AIP Publishing LLC.

# Cathodoluminescence microscopy and spectroscopy of GaN epilayers microstructured using surface charge lithography

C. Díaz-Guerra[a] and J. Piqueras
*Departamento de Física de Materiales, Facultad de Ciencias Físicas, Universidad Complutense de Madrid, E-28040 Madrid, Spain*

O. Volciuc, V. Popa, and I. M. Tiginyanu
*Laboratory of Low-Dimensional Semiconductor Structures, Institute of Applied Physics, Academy of Sciences of Moldova, 2028 Chisinau, Moldova and National Center for Materials Study and Testing, Technical University of Moldova, 2004 Chisinau, Moldova*

(Received 13 February 2006; accepted 8 May 2006; published online 19 July 2006)

Cathodoluminescence (CL) microscopy and spectroscopy have been used to investigate the optical properties of GaN microstructures patterned by $Ar^+$ ion irradiation and subsequent photoelectrochemical (PEC) etching. Monochromatic CL images and CL spectra reveal an enhancement of several defect-related emission bands in a 10 $\mu$m wide area around each microstructure. In addition, columnar nanostructures and nanoetch pits were found in the PEC etched areas. CL emission of the nanocolumns is dominated by free electron to acceptor transitions, while excitonic luminescence prevails in the rest of the etched GaN layers. Investigation of the sidewalls of the microstructures reveals that a CL emission band centered at about 3.41 eV, attributed to excitons bound to structural defects, is effectively suppressed after PEC etching only in the observed nanocolumns. © *2006 American Institute of Physics*. [DOI: 10.1063/1.2214210]

## I. INTRODUCTION

GaN and related ternary alloys are important wide band gap semiconductors for a broad range of applications as high-frequency/high-temperature electronics and visible and ultraviolet emitters and detectors. Further improvement in device performance hinges on several factors, including understanding and reduction of point and extended defects and the development of micro- and nanoscale patterning techniques. Etching of these materials, which is an important process for the fabrication of optimal device structures, is difficult due to their chemical inertness. However, photoelectrochemical (PEC) etching, encompassing light-induced electrochemical reactions of semiconductors in contact with liquids, has been shown to be capable of rapid,[1] dislocation-selective,[2] dopant-selective,[3] or band-gap-selective[4] etchings of GaN and related ternary compounds. In addition, different kinds of nanostructures, such as nanowires and nanocolumns, have been fabricated by PEC etching of thin GaN films and related to the dislocation structure of the samples.[5]

The observation that mechanical damage inhibited the PEC etching of GaAs, led Yamamoto and Yano[6] to pattern the surface of *n*-GaAs wafers for selective material removal with the damage induced by ion bombardment. Such damage inhibited subsequent PEC etching by enhancing the recombination rate of the photogenerated holes in the irradiated areas. The method was then extended to pattern *n*-type GaAs, InP, InGaAs, and InGaAsP by direct writing with a focused ion beam.[7–9] Recently, fabrication of GaN microstructures following a similar approach has been reported.[10] Defects created at the surface of *n*-type GaN films using an Ar ion beam lead to the formation of a layer of trapped negative surface charge shielding the material against PEC etching. This surface charge can be exploited as a lithographic mask for cost-effective manufacturing of GaN microstructures.

In the present work, cathodoluminescence (CL) in the scanning electron microscope (SEM) has been applied to investigate the effects of irradiation and subsequent PEC etching processes in the optical and structural properties of undoped GaN films. CL measurements reveal that the effects of irradiation extend to a 10 $\mu$m wide region that surrounds the microstructures patterned following the procedure described above. Furthermore, a direct correlation between the morphology and the radiative recombination properties of individual nanostructures created after PEC etching in such region has also been established.

## II. EXPERIMENT

GaN layers used were grown by low-pressure metalorganic chemical vapor deposition (MOCVD) on sapphire substrates. A buffer layer of 20 nm thick GaN was first grown at 510 °C. Subsequently, a 2 $\mu$m thick, nominally undoped, top GaN layer was grown at 1100 °C. The concentration of free electrons in the top layer was $1.8\times10^{17}$ $cm^{-3}$. Selected areas of the samples were irradiated using 2 keV $Ar^+$ ions at a fluence of $3\times10^{12}$ $cm^{-2}$. PEC etching was carried out in a stirred 0.1 M aqueous solution of KOH for 10 min under *in situ* ultraviolet illumination provided by a 200 W Xe lamp focused on the GaN surface exposed to the electrolyte. No bias was applied to the sample during etching.

The morphology of the samples was studied using a Leica 440 Stereoscan SEM or a Jeol JSM-6335F field emission SEM (FSEM). CL investigations were carried out in a

[a]Electronic mail: cdiazgue@fis.ucm.es

 

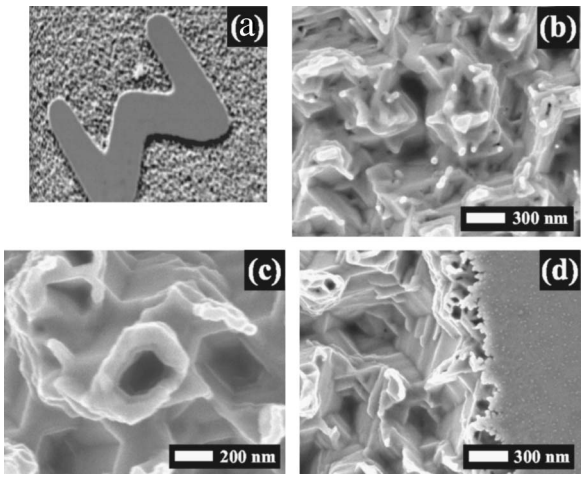


FIG. 1. SEM image of a microstructure ("M" letter) fabricated by ion irradiation and subsequent PEC etching (a) and top-view FSEM images [(b)–(d)] of the surrounding PEC etched material.

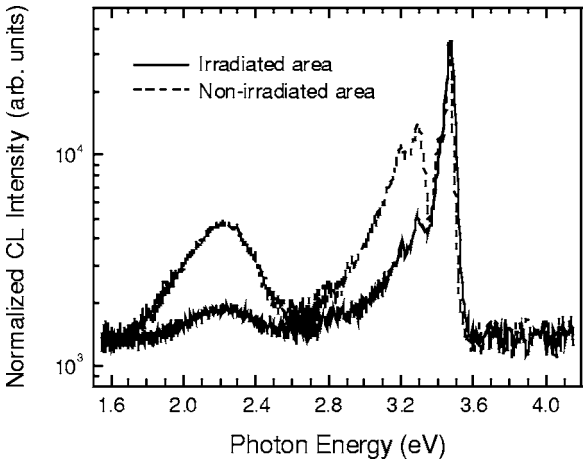


FIG. 2. CL spectra (87 K, 10 kV) from a PEC etched GaN sample recorded in areas irradiated (solid line) and nonirradiated (dashed line) with $Ar^+$ ions before etching.

Hitachi S-2500 SEM and a Leica 440 SEM. Measurements were performed at accelerating voltages ranging from 5 to 15 kV, beam currents ranging from 0.5 to 6 nA and temperatures between 85 and 295 K. CL spectra were recorded using a charge-coupled device (CCD) camera with a built-in spectrograph (Hamamatsu PMA-111) or a Hamamatsu R928P photomultiplier working in the photon counting mode and a computer controlled Oriel 74100 monochromator. The chemical composition of the samples was investigated by wavelength dispersive x-ray (WDX) microanalysis in a Jeol JXA-8900M Superprobe using an accelerating voltage of 10 kV.

## III. RESULTS AND DISCUSSION

Figure 1(a) shows a SEM image of a GaN layer where a "mesalike" microstructure ("M" letter) has been patterned by ion irradiation and subsequent PEC etching. A selection of high-resolution top-view FSEM images taken at several magnifications in the surrounding area of such microstructure is shown in Figs. 1(b)–1(d). The top of the mesa shows a very smooth appearance, which confirms that etching is not effective on the irradiated areas. On the contrary, a channellike structure with terraces at different heights can be observed in the PEC etched, not previously irradiated, layer [Fig. 1(b)]. The average width of the channels is ~500 nm. Columnar structures of irregular shapes and heights, some of them hollow—showing a chimney appearance—separate the channels. Hexagonal etch pits (100–400 nm in size) can be appreciated at the bottom of the channels and inside the chimneys [Fig. 1(c)]. The border between the irradiated areas (letters) and the PEC etched material is shown in Fig. 1(d). The morphology here described does not depend on the area, close or far away from the irradiated regions, of the examined PEC etched GaN layers.

CL spectra at different temperatures and excitation densities were recorded in areas irradiated and nonirradiated with $Ar^+$ ions before etching. Figure 2 illustrates the results obtained at 87 K using an accelerating voltage of 10 kV (scanned area $\sim 50 \times 50\ \mu m^2$). The spectral distribution of the CL emission exhibits peaks in the visible and the UV ranges. In the low energy region, the so-called yellow band is observed centered at about 2.22 eV. Gaussian deconvolution of the obtained spectra (not shown) reveals that two bands—respectively centered at about 2.26 and 2.07 eV—contribute to this deep-level luminescence, although no significant difference in the spatial distribution of both bands was found in the investigated areas. According to recent time-resolved PL and CL studies, the emissions contributing at 87 K to this complex band can be attributed to radiative transitions from the conduction band to deep acceptor levels containing Ga vacancies.[11–13] The intensity of the complex yellow band is weak in the irradiated areas and higher in the PEC etched regions. In the second group of peaks, an intense CL band appears centered at 3.287 eV. This emission is related to electron transitions from the conduction band to shallow acceptors ($eA^0$ transitions) (Refs. 13–15) and is observed as the dominant emission in CL spectra recorded from PEC etched areas at high magnification. The peaks centered at about 3.200 and 3.108 eV correspond, respectively, to the first and second LO phonon replicas of the $eA^0$ transition. $C_N$ and $Mg_{Ga}$ have been proposed[14,15] as the acceptor involved in this emission, although there is an increasing experimental evidence supporting $Si_N$ as the shallow acceptor responsible for the $eA^0$ band.[13] CL spectra recorded at different temperatures indicate that the $eA^0$ emission is quenched above 180 K with an activation energy of about 175 meV.

The peak observed at higher energy corresponds to GaN near band edge luminescence. Irrespective of the growth method, shallow donor ionization in GaN is almost complete at 87 K and the near band gap luminescence is dominated by the free exciton A (FXA) transition.[14,16,17] In strain-free samples, the FXA transition is peaked at 3.471 eV for $T = 87$ K.[14,16] However, the thermal expansion mismatch between GaN and the sapphire substrate strains the GaN layer. This biaxial compressive strain decreases as the layer thickness increases.[18] The compressive strain blueshifts the free exciton peak position, while the tensile stress, as that inherent to thin GaN layers grown on SiC substrates, redshifts the free exciton peak. The free exciton emission in the irradiated

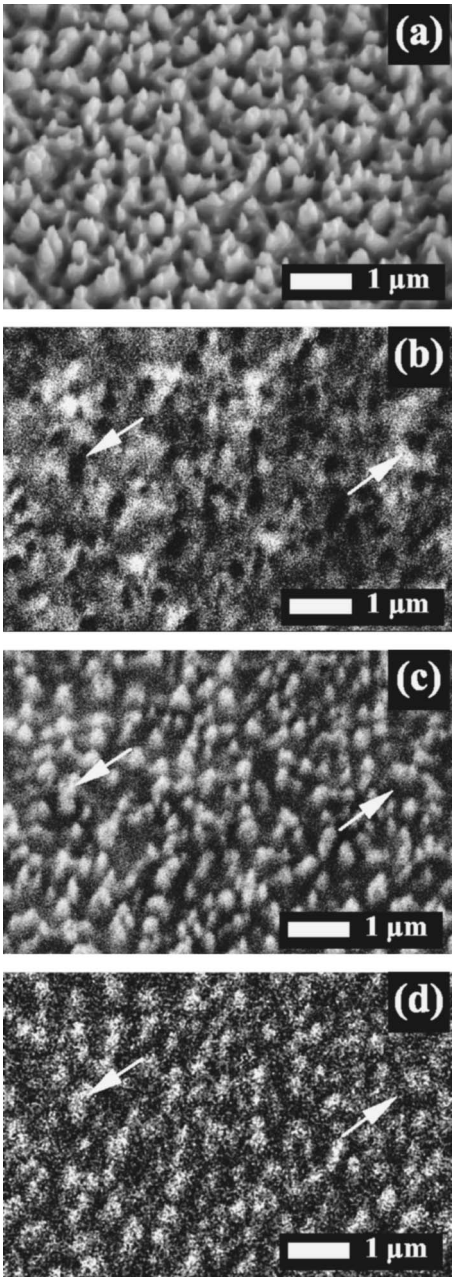


FIG. 3. Secondary electron micrograph (a) and corresponding monochromatic CL images [(b)–(d)] from an etched area close to one of the patterned microstructures. CL micrographs were respectively recorded at (b) 3.46 eV (358 nm), (c) 3.28 eV (378 nm), and (d) 2.26 eV (549 nm). Arrows indicate equivalent positions in the images.

areas is peaked at 3.478 eV. According to the models proposed in the literature,[19] this evidences the occurrence of an average biaxial stress of about 0.2 GPa. On the contrary, CL spectra recorded on PEC etched regions shows a FXA peak at 3.462 eV, indicating the existence of a tensile stress of about 0.33 GPa.[19]

In order to visualize the spatial distribution of the above described emission bands, monochromatic CL images were recorded at the corresponding peak energies. Figure 3 shows results obtained in a PEC etched area close to one of the patterned microstructures. The CL micrograph recorded at 3.46 eV (band gap luminescence) shows that such emission is enhanced in the areas between the nanocolumns [Fig. 3(b)], while the image recorded at 3.28 eV [Fig. 3(c)]—corresponding to the $eA^0$ band—shows the opposite contrast. In addition, a clear correlation between the monochromatic CL image recorded at 2.26 eV [Fig. 3(d)], related to the yellow emission, and that showing the spatial distribution of the $eA^0$ band can be clearly appreciated. Actually, the intensity of the yellow luminescence (YL) is higher in the same points where an enhanced $eA^0$ emission is observed. Representative CL spectra recorded at high magnification on the column tips and the etch pits are shown in Fig. 4. Close to the exciton peak, an emission centered near 3.41 eV can be observed in CL spectra from the etch pits. The origin of this band will be discussed later on. The intensity of the $eA^0$ band relative to the exciton emission is higher on the columns and the same applies for the yellow emission. Such trend was observed in all the spectra recorded in the sample. In fact, measurements over 20 spectra recorded on nonirradiated areas reveal that the ratio between the intensity of the exciton emission and that of the $eA^0$ band is $(0.19\pm0.04)$ on the top of the nanocolumns and $(0.36\pm0.05)$ in the pits, while the ratio between the intensity of the YL and that of the exciton peak is $\sim 0.35$ in the pits and varies between 0.7 and 1.5 on the column tips.

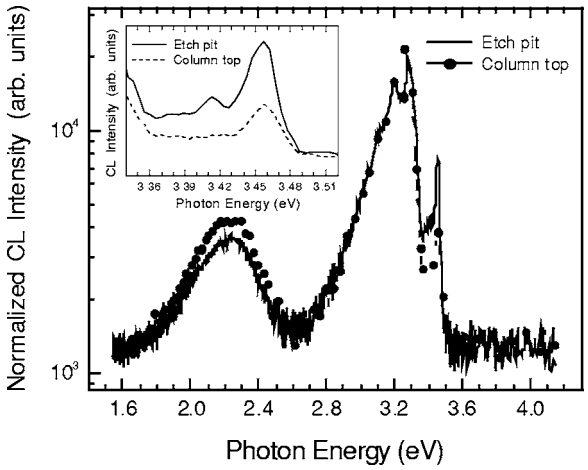


FIG. 4. CL spectra (87 K, 8 kV) from a PEC etched GaN sample recorded on top of the columns and on the etch pits. The inset shows a detail of the near band-gap emission bands.

Since the relative intensities of the CL emission bands observed in spectra from nonirradiated and irradiated parts of the layer are clearly different, as shown in Fig. 2, monochromatic CL images were also recorded in areas including patterned microstructures. An example is shown in Fig. 5. The near band gap emission is higher in the areas irradiated prior to etching [Fig. 5(b)], while both the intensity of the $eA^0$ band [(Fig. 5(c)] and the intensity of the YL [Fig. 5(d)] are much lower in the same regions. In addition, the latter micrographs reveal an enhancement of the $eA^0$ and the YL in the surroundings of the irradiated zones (letter "O"). Such enhancement gives rise in the related monochromatic CL images to a bright halo that spreads approximately 10 $\mu$m from the edge of the mentioned areas. Spectra representative from the three regions (irradiated, nonirradiated, and halos) are shown in Fig. 5(e). Both the intensity of the YL and especially the intensity of the $eA^0$ emission are higher in the halo surrounding the microstructure. These observations sug-

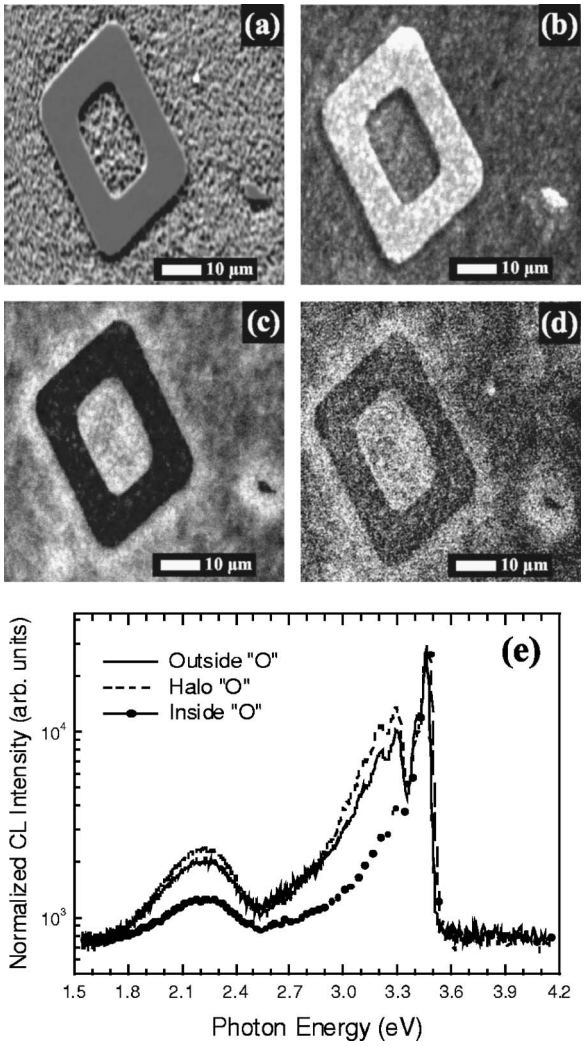


FIG. 5. Secondary electron image (a) and corresponding monochromatic CL images (87 K, 10 kV) recorded at (b) 3.46 eV (358 nm), (c) 3.28 eV (378 nm), and (d) 2.26 eV (549 nm) from a region of a GaN layer containing nonirradiated and irradiated (letter "O") areas. (e) CL spectra recorded outside, inside, and in the surroundings of the microstructure.

gest an increased concentration of the acceptors levels responsible for the observed emissions in such area, as compared with the rest of the PEC etched material. Si and O are common impurities found in nominally undoped GaN films. In order to check if compositional inhomogeneities might account for the halos observed in our CL images, Ga, N, Si, and O WDX mappings were recorded in the same area shown in Fig. 5. Almost no contrast was observed in Si and O compositional images, while homogeneous Ga and N spatial distributions were found in the irradiated areas. Nevertheless, the Ga concentration measured on top of these microstructures was found to be ~3% higher than the average Ga content measured in the PEC etched, nonirradiated material. However, halos similar to those observed in monochromatic CL images were not observed in any of the obtained WDX mappings. It has been previously reported that conductivity of GaN is increased by preferential loss of N during 2.5 keV $Ar^+$ irradiation.[20] The surface oxygen concentration also increases after the same treatment. Depletion of nitrogen leaves excess metallic Ga on the surface. This change in stoichiometry renders the surface highly *n* type due to the increased concentration of nitrogen vacancies ($V_N$), which act as shallow donors in GaN. Similar compositional changes have been observed in reactively ion etched GaN surfaces[21] or GaN surfaces subjected to neutral Ar plasmas.[22] The PEC etch process is very sensitive to the spatial distribution of charges at the semiconductor surface. An excess of negative free charge can reduce the effective number of photogenerated holes available for the subsequent etching process. Actually, an enhanced near band-edge luminescence is observed in the irradiated areas after PEC etching [see Fig. 5(a)]. Besides creation of nonstoichiometric surfaces due to preferential depletion of one of the elements, irradiation creates near-surface defects, which can diffuse deeper into the sample. In fact, SRIM (Ref. 23) simulations predict an ion distribution depth of about 4 nm for 2 keV $Ar^+$ ions at normal incidence for GaN. However, there is experimental evidence of large damage propagation in this material through ion channeling and diffusion mechanisms even for much lower $Ar^+$ ion energies.[24,25] Our CL results indicate a clear decrease of the shallow acceptors responsible for the 3.287 eV emission, as evidenced by the monochromatic CL images obtained at this energy and the CL spectra from the irradiated regions shown in Fig. 5. Moreover, it seems that irradiation does not significantly increase the concentration of Ga vacancies in the present case, since we observed no enhancement of the yellow luminescence in the areas exposed to the ion beam. Our CL measurements also reveal an enhanced YL and $eA^0$ emission in a wide halo surrounding the irradiated areas. Khare and Hu[26] reported that PEC etching was suppressed in ion irradiated *n*-GaAs not only in the implanted region but also within a region extending a few microns beyond the implanted region. Calculations suggested that the diffusion of the photogenerated hole carriers, relative to their reaction rate at the surface, was the parameter that determined the extension of the damaged area. Space charge region effects as well as a possible lateral electric field between the irradiated ($n^+$ material) and nonirradiated regions were not taken into account but may also play an important role in the case of the GaN sample here investigated. Although no morphological changes were observed in the material close to the irradiated GaN regions, CL results indicate that the influence of $Ar^+$ ions irradiation extends up to about 10 $\mu$m from the exposed areas. The strong enhancement of the YL and $eA^0$ emissions suggests an increased concentration of the acceptors responsible for these bands; shallow acceptors in the first case and deep acceptors ($V_{Ga}$ containing complexes such as $V_{Ga}O_N$ or $V_{Ga}Si_{Ga}$) in the second one.

Finally, the morphology and luminescence properties of the lateral walls of the microstructures fabricated by ion treatment and subsequent PEC etching were investigated by SEM and CL spectroscopy. Figures 6(a) and 6(b) show SEM images of the sidewalls of two different irradiated zones. Close to the top of such regions a columnar structure can be appreciated but roughness clearly decreases as we move towards the bottom. CL spectra recorded at regular intervals along a lateral wall, as well as on the top of the mesa and the etched film are shown in Fig. 6(c). Position 1 is located on top of the mesa, positions 2–4 are on the sidewall, and posi-

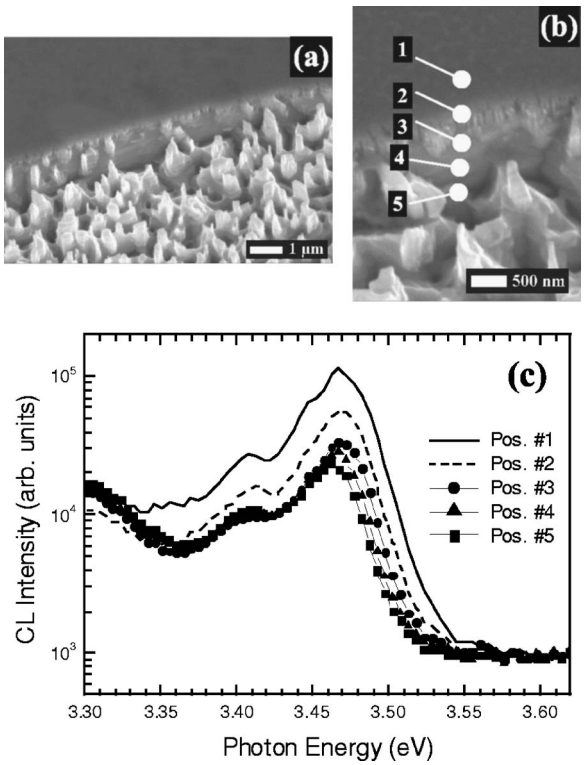


FIG. 6. SEM images [(a) and (b)] of the sidewalls of two different microstructures. The white lines in (b) mark the points where CL spectra shown in (c) were recorded ($T$=87 K, 8 kV).

tion 5 corresponds to a pit in the PEC etched layer. Careful inspection of the near band edge CL emission reveals the existence of a band peaked near 3.41 eV [Fig. 6(c)]. The absolute intensity of this band is higher on the top and close to the top of the mesa (positions 1 and 2) and remains almost constant on the other positions of the sidewall considered. An emission centered at the same energy has been previously observed in both undoped and Si-doped GaN layers and attributed to excitons bound to structural defects such as dislocations[27,28] or stacking faults.[29] Nonspatially resolved PL studies carried out by Reschikov *et al.*[30] in undoped GaN films grown by MBE revealed that the 3.41 eV emission almost completely disappeared after PEC etching, what lead the mentioned authors to suggest that the associated defect was at the GaN surface. The situation is similar for the MOCVD grown material investigated here, but our spatially resolved CL measurements indicate that the scenario is somehow more complicated. A certain decrease of the 3.41 eV emission intensity is observed along the sidewall of the microstructures, but such band can still be clearly appreciated in CL spectra from the PEC etched layer [Fig. 6(c), position 5]. However, the latter spectrum was recorded in a region were nanocolumns were not present. Comparison of CL spectra shown in Fig. 4 (see inset) reveals that the 3.41 eV emission is effectively suppressed after PEC etching in the nanocolumns but not in the rest of the etched material.

## IV. CONCLUSIONS

In summary, surface charge lithography, based on the formation of a layer of trapped negative surface charge shielding the material against PEC etching, has been used for manufacturing of GaN microstructures. The optical and structural properties of both the fabricated microstructures and the PEC etched material have been assessed by CL microscopy and spectroscopy. CL measurements reveal that the effects of $Ar^+$ ion irradiation and subsequent PEC etching extend to a 10 $\mu$m wide halo surrounding each microstructure. A clear enhancement of the emission bands related to both shallow and deep acceptor levels was observed in the halos, where no compositional changes were detected by WDX microanalysis.

Besides, columnar nanostructures and nanoetch pits were found in the PEC etched areas located either close or far from the patterned microstructures. CL emission of the nanocolumns is dominated by free electron to acceptor transitions, while excitonic luminescence prevails in the rest of the etched GaN layers. Investigation of the sidewalls of the microstructures reveal that a CL emission band centered at about 3.41 eV, attributed to excitons bound to structural defects, is effectively suppressed after PEC etching only in the observed nanocolumns.

## ACKNOWLEDGMENTS

This work has been supported by MEC through Project No. MAT2003-00455, CAM through Project GR/MAT 630-04, U.S. Civilian Research and Development Foundation under Grant Nos. MR2-995 and MOR2-1033-CH-03, as well as by the Supreme Council for Research and Technological Development of Moldova.

[1] C. Youtsey, I. Adesida, and G. Bulman, Appl. Phys. Lett. **71**, 2151 (1997).
[2] C. Youtsey, L. T. Romano, and I. Adesida, Appl. Phys. Lett. **73**, 797 (1998).
[3] A. R. Stonas, P. Kozodoy, H. Marchand, P. Fini, S. P. DenBaars, U. K. Mishra, and E. L. Hu, Appl. Phys. Lett. **77**, 2610 (2000).
[4] A. R. Stonas, T. Margalith, S. P. DenBaars, L. A. Coldren, and E. L. Hu, Appl. Phys. Lett. **78**, 1945 (2001).
[5] C. Díaz-Guerra, J. Piqueras, V. Popa, A. Cojocaru, and I. M. Tiginyanu, Appl. Phys. Lett. **86**, 223103 (2005).
[6] A. Yamamoto and S. Yano, J. Electrochem. Soc. **122**, 260 (1975).
[7] A. Yamamoto, S. Thono, and C. Uemura, J. Electrochem. Soc. **128**, 1095 (1981).
[8] G. C. Chi, F. W. Ostermayer, K. D. Cummings, and L. R. Harriot, J. Appl. Phys. **60**, 4012 (1986).
[9] K. D. Cummings, L. R. Harriot, G. C. Chi, and F. W. Ostermayer, Appl. Phys. Lett. **48**, 659 (1986).
[10] I. M. Tiginyanu, V. Popa, and O. Volciuc, Appl. Phys. Lett. **86**, 174102 (2005).
[11] M. A. Reshchikov, H. Morkoç, S. S. Park, and K. Y. Lee, Appl. Phys. Lett. **78**, 2882 (2001).
[12] C. Díaz-Guerra, J. Piqueras, and A. Cavallini, Appl. Phys. Lett. **82**, 2050 (2003).
[13] M. A. Reshchikov and H. Morkoç, J. Appl. Phys. **97**, 061301 (2005), and references therein.
[14] M. Leroux, N. Greandjean, B. Beaumont, G. Nataf, F. Semond, J. Massies, and P. Gibart, J. Appl. Phys. **86**, 3721 (1999).
[15] M. A. Reshchikov, D. Huang, F. Yun, L. He, H. Morkoç, D. C. Reynolds, S. S. Park, and K. Y. Lee, Appl. Phys. Lett. **79**, 3779 (2001).
[16] F. Calle, F. J. Sánchez, J. M. G. Tijero, M. A. Sánchez-García, E. Calleja, and R. Beresford, Semicond. Sci. Technol. **12**, 1396 (1997).
[17] G. Martínez-Criado, C. R. Miskys, A. Cros, O. Ambacher, A. Cantarero, and M. Stutzman, J. Appl. Phys. **90**, 5627 (2001).
[18] D. C. Reynolds, D. C. Look, B. Jogai, J. E. Hoelscher, R. E. Sherriff, and R. J. Molnar, J. Appl. Phys. **88**, 1460 (2000).
[19] C. Kisielowski *et al.*, Phys. Rev. B **54**, 17745 (1996).

[20]K. S. A. Butcher, P. Afifuddin, T. L. Tansley, N. Brack, P. J. Pigram, H. Timmers, K. E. Princed, and R. G. Elliman, Appl. Surf. Sci. **230**, 18 (2004).
[21]J. Y. Chen, C. J. Pan, and G. C. Chi, Solid-State Electron. **43**, 649 (1999).
[22]R. Cheung, R. J. Reeves, S. A. Brown, E. van der Drift, and M. Kamp, J. Appl. Phys. **88**, 7110 (2000).
[23]J. F. Ziegler and J. P. Biersack, Stopping and Range of Ions into Matter (SRIM) software. http://www.srim.org/
[24]E. D. Haberer, C. H. Chen, A. Abare, M. Hansen, S. DenBaars, L. Coldren, U. Mishra, and E. L. Hu, Appl. Phys. Lett. **76**, 3941 (2000).
[25]E. D. Haberer, C. H. Chen, M. Hansen, S. Keller, S. DenBaars, L. Coldren, U. K. Mishra, and E. L. Hu, J. Vac. Sci. Technol. B **19**, 603 (2001).
[26]R. Khare and E. Hu, J. Appl. Phys. **72**, 1543 (1992).
[27]E. Calleja, M. A. Sánchez-García, F. J. Sánchez, F. Calle, F. B. Naranjo, E. Muñoz, U. Jahn, and K. Ploog, Phys. Rev. B **62**, 16826 (2000).
[28]C. Trager-Cowan, S. McArthur, P. G. Middleton, K. P. O'Donnell, D. Zubia, and S. D. Hersee, MRS Internet J. Nitride Semicond. Res. **3**, 36 (1998).
[29]S. Fisher *et al.*, J. Cryst. Growth **189–190**, 556 (1998).
[30]M. A. Reschikov, D. Huang, F. Yun, H. Morkoç, R. J. Molnar, and C. W. Litton, Mater. Res. Soc. Symp. Proc. **693**, I6.28 (2002).